Vibration Control of Spacecraft Box Structures Using a Collocated Piezo-actuator/Sensor

C. J. DAMAREN[1,*] AND D. C. D. OGUAMANAM[2]

[1]*Institute for Aerospace Studies, University of Toronto, 4925 Dufferin Street, Toronto, ON M3H 5T6, Canada*
[2]*Department of Mechanical and Industrial Engineering, Ryerson University, 350 Victoria Street, Toronto, ON M5B 2K3, Canada*

ABSTRACT: The problem of vibration control in box-type structures is examined by inclusion of piezo-electric smart structural elements. The box is modeled as a system of joined plates in which both extensional and bending deflections are incorporated. By collocating the sensor and actuator elements, the input–output property of passivity is achieved independent of the number of modeled modes and details such as frequencies and mode shapes. Robust vibration control is achieved by designing a strictly positive real dynamic compensator for the system.

Key Words: smart structures, box structures, collation, strictly positive real

INTRODUCTION

THE applications of layers of piezo-electric materials to thin-walled elastic structures offers the ability to introduce active damping in a distributed fashion (Crawley and de Luis, 1987). By physically collocating such "smart" materials configured as dual sensors and actuators, the important input–output property of passivity is achieved. This property is independent of the details of the mass and stiffness distributions and provides a mechanism for robust stabilization via the passivity theorem. This important result in input–output theory (Desoer and Vidyasagar, 1975) states that any strict passivity operator connected in negative feedback with a passive system yields input–output stability.

Linear time-invariant (LTI) passive systems are characterized by positive real transfer functions. In the context of flexible structures, the positive real property is independent of the number of vibration modes in the model as well as the details of the mode shapes and natural frequencies. Hence, any strictly passive feedback yields robust stability since spillover instabilities, which can result from controller designs based on a reduced subset of modes, are avoided. LTI controllers which are strictly passive are closely related to the strictly positive real (SPR) property (Wen, 1988). In particular, any SPR feedback always stabilizes a passive system.

The use of dynamic SPR compensation for stabilization of large space structures was suggested by Benhabib et al. (1981). Since then, several authors have presented systematic methodologies for designing SPR control. In this work, we adopt the technique of Lozano-Leal and Joshi (1988) who demonstrated LQG weight selection such that the Kalman-Yakubovich Lemma was satisfied, i.e., the LQG controller is SPR.

Small satellites have been increasing in importance given the need to reduce spacecraft design costs. Reduction in size and mass while continuing to require tight performance objectives leads to active vibration control as a possible design alternative. Microspacecraft structures are typically simplistic in design and consist of homogeneous materials arranged in simple geometries. A box or stack of trays are common approaches.

Although many authors have looked at control using of "smart" structural elements in beam (Bailey and Hubbard, 1985; Halim and Moheimani, 2002) and plate structures (Baz and Ro, 1996; Sun et al., 2001; Wang et al., 2001), the box architecture has escaped notice. In addition to the small satellite application, this is a relatively simple structure with interesting but non-trivial vibration mode shapes. This paper examines the vibration control of box-type structures using a collocated piezo-actuator/sensor combination in conjunction with SPR control.

MOTION EQUATIONS

A schematic of a box structure is shown in Figure 1 along with the global axes $\{X, Y, Z\}$ and corresponding deflections $\{U, V, W\}$ and rotations $\{\Theta_x, \Theta_y, \Theta_z\}$. Each side of the box is modeled as a thin plate.

A local coordinate frame is selected such that (x, y) lies in the plane of the plate and z is aligned with the surface normal. The x- and y-axes are parallel to the sides of the plate. The corresponding extensional deflections of the midplane are $[u_0(x, y, t), v_0(x, y, t)]$

*Author to whom correspondence should be addressed.
Email: damaren@utias.utoronto.ca

1045-389X/04/05 0369–6 $10.00/0 DOI: 10.1177/1045389X04040901

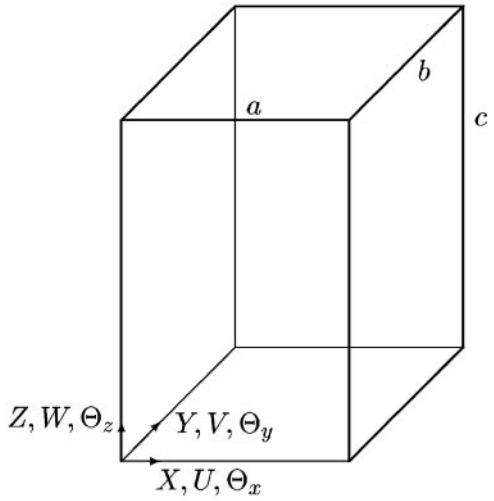

Figure 1. *Box structure schematic.*

and the normal deflection is $w(x, y, t)$. For a homogeneous isotropic box of mass density ρ and panel thickness h, thin-plate theory gives the corresponding kinetic and potential energies for each plate as

$$T = \frac{1}{2}\rho h \iint_S \left[\left(\frac{\partial u_0}{\partial t}\right)^2 + \left(\frac{\partial v_0}{\partial t}\right)^2 + \left(\frac{\partial w}{\partial t}\right)^2 \right] dx\, dy \quad (1)$$

$$\begin{aligned} V = {} & \frac{1}{2} D \iint_S \left[\left(\frac{\partial^2 w}{\partial x^2}\right)^2 + \left(\frac{\partial^2 w}{\partial y^2}\right)^2 + 2\nu \frac{\partial^2 w}{\partial x^2}\frac{\partial^2 w}{\partial y^2} \right. \\ & \left. + 2(1-\nu)\left(\frac{\partial^2 w}{\partial x \partial y}\right)^2 \right] dx\, dy \\ & + \frac{1}{2} C \iint_S \left[\left(\frac{\partial u_0}{\partial x}\right)^2 + \left(\frac{\partial v_0}{\partial y}\right)^2 + 2\nu \frac{\partial u_0}{\partial x}\frac{\partial v_0}{\partial y} \right. \\ & \left. + \frac{1-\nu}{2}\left(\frac{\partial u_0}{\partial y} + \frac{\partial v_0}{\partial x}\right)^2 \right] dx\, dy \end{aligned} \quad (2)$$

where E is Young's modulus, ν is Poisson's ratio, $D = Eh^3/[12(1-\nu^2)]$ is the bending rigidity, and $C = Eh/(1-\nu^2)$ is the extensional rigidity.

For spatial discretization, rectangular finite elements are used with the following expansions within each element:

$$u_0(\hat{x}, \hat{y}, t) = [1 \;\; \hat{x} \;\; \hat{y} \;\; \hat{x}\hat{y}]\mathbf{A}_u \mathbf{q}_u(t) \quad (3)$$

$$v_0(\hat{x}, \hat{y}, t) = [1 \;\; \hat{x} \;\; \hat{y} \;\; \hat{x}\hat{y}]\mathbf{A}_v \mathbf{q}_v(t) \quad (4)$$

$$\begin{aligned} w(\hat{x}, \hat{y}, t) = {} & [1 \;\; \hat{x} \;\; \hat{y} \;\; \hat{x}^2 \;\; \hat{x}\hat{y} \;\; \hat{y}^2 \;\; \hat{x}^3 \;\; \hat{x}^2\hat{y} \;\; \hat{x}\hat{y}^2 \;\; \hat{y}^3 \;\; \hat{x}^3\hat{y} \;\; \hat{x}\hat{y}^3] \\ & \times \mathbf{A}_w \mathbf{q}_w(t) \end{aligned} \quad (5)$$

Here, $(\hat{x}, \hat{y}) \in [0,1] \times [0,1]$ are nondimensionalized local coordinates and $\mathbf{A}_u$, $\mathbf{A}_v$, $\mathbf{A}_w$ are constant matrices evaluated so that $\mathbf{q}_u$, $\mathbf{q}_v$, and $\mathbf{q}_w$ contain prescribed nodal degrees of freedom at the element corners. In the case of $\mathbf{q}_u$ and $\mathbf{q}_v$ these are simply the four corresponding displacements and in the case of $\mathbf{q}_w$, they are the corner values of $\{w, \partial w/\partial x, \partial w/\partial y\}$. The global vector of degrees of freedom, $\mathbf{q}$, contains the assembly of nodal degrees of freedom which are the three displacements and rotations $\{U, V, W, \Theta_x, \Theta_y, \Theta_z\}$ and is readily constructed from simple transformations of $\mathbf{q}_u$, $\mathbf{q}_v$, and $\mathbf{q}_w$. With the above expansions, the energies take on the familiar forms $T = (1/2)\dot{\mathbf{q}}^T \mathbf{M} \dot{\mathbf{q}}$ and $V = (1/2)\mathbf{q}^T \mathbf{K} \mathbf{q}$ with symmetric matrices $\mathbf{M}$ and $\mathbf{K}$.

We assume that a single piezo-electric sensor is located on the structure whose area coincides with a single finite element. The corresponding piezo-actuator is collocated with it. It is assumed that the sensor and actuator are mounted on the same side of the plate and contribute negligible mass and stiffness.

Following Lee (1990), the current created by the piezo-sensor is $y(t) = dq_s/dt$ where the sensor charge is

$$\begin{aligned} q_s = \iint_S F(x,y) P_0(x,y) \left\{ \left[e_{31}^0 \frac{\partial u_0}{\partial x} + e_{32}^0 \frac{\partial v_0}{\partial y} \right] \right. \\ \left. - z_k^0 \left[e_{31}^0 \frac{\partial^2 w}{\partial x^2} + e_{32}^0 \frac{\partial^2 w}{\partial y^2} \right] \right\} dx\, dy \end{aligned} \quad (6)$$

where e_{31}^0 and e_{32}^0 are the piezo-electric charge constants, $F(x, y) = 1$ if (x, y) contains sensor electrodes and vanishes otherwise, and $P_0(x, y)$ expresses the polarization profile which is taken to be identically unity here. The height of the layer above the plate's neutral axis is $z_k^0 = h/2$ where we have neglected the sensor and actuator thickness. Assuming uniform polarization within a rectangular patch area $S_p = [x_1, x_2] \times [y_1, y_2]$, we have

$$\begin{aligned} F(x,y)P_0(x,y) = {} & [H(x - x_1) - H(x - x_2)] \\ & \times [H(y - y_1) - H(y - y_2)] \end{aligned}$$

where $H(x)$ is the Heaviside step function. Substituting the expansions in Equations (3)–(5) into (6) leads to the output equation

$$y(t) = \mathbf{c}^T \dot{\mathbf{q}} \quad (7)$$

where $\mathbf{c}$ is a constant column vector.

The virtual work stemming from a collocated actuator is readily constructed from Lee (1990) as

$$\begin{aligned} \delta W_e = - \iint_S \delta_{ep} u(t) \left[e_{31}^0 \frac{\partial (FP_0)}{\partial x} \delta u_0 + e_{32}^0 \frac{\partial (FP_0)}{\partial y} \delta v_0 \right. \\ \left. + z_k^0 e_{31}^0 \frac{\partial^2 (FP_0)}{\partial x^2} \delta w + z_k^0 e_{32}^0 \frac{\partial^2 (FP_0)}{\partial y^2} \delta w \right] dx\, dy \end{aligned} \quad (8)$$

where $u(t)$ is the applied voltage and $\delta_{ep} = 1$ if the electric field and poling direction point in the same

direction. Substituting the expansions, Equations (3)–(5), into the above and recognizing the duality between Equations (6) and (8) leads to $\delta W_e = \delta \mathbf{q}^T \mathbf{b} u(t)$ where $\mathbf{b} = \mathbf{c}$. Applying Hamiltons principle to the energy and work expressions leads to the standard motion equations

$$\mathbf{M}\mathbf{q} + \mathbf{K}\mathbf{q} = \mathbf{b}u(t) \tag{9}$$

MODAL ANALYSIS AND CONTROLLER DESIGN MODEL

The eigenproblem corresponding to (9) is

$$-\omega_\alpha^2 \mathbf{M}\mathbf{q}_\alpha + \mathbf{K}\mathbf{q}_\alpha = \mathbf{0}, \quad \alpha = 1, 2, 3, \ldots$$

where ω_α are the undamped vibration frequencies with corresponding eigenvectors $\mathbf{q}_\alpha$ normalized so that $\mathbf{q}_\alpha^T \mathbf{M} \mathbf{q}_\beta = \delta_{\alpha\beta}$. There are also six zero-frequency rigid body modes which are neglected in the subsequent analysis since they are unobservable and uncontrollable using the proposed actuator and sensor. The modal expansion $\mathbf{q}(t) = \sum_\alpha \mathbf{q}_\alpha \eta_\alpha(t)$ introduced into (9) leads to uncoupled motion equations of the form

$$\begin{aligned} &\ddot{\eta}_\alpha + 2\zeta_\alpha \omega_\alpha \dot{\eta}_\alpha + \omega_\alpha^2 \eta_\alpha = \hat{b}_\alpha u(t), \\ &\hat{b}_\alpha = \mathbf{q}_\alpha^T \mathbf{b}, \quad \alpha = 1, 2, 3, \ldots \end{aligned} \tag{10}$$

where we have taken the liberty of introducing light structural damping in the form of modal damping factors ζ_α. Substituting the modal expansion into the output equation in (7) leads to

$$y(t) = \sum_\alpha \hat{c}_\alpha \dot{\eta}_\alpha, \quad \hat{c}_\alpha = \hat{b}_\alpha \tag{11}$$

for the sensor measurement. Taking Laplace transforms in Equations (10) and (11) leads to the transfer function

$$y(s)/u(s) = \sum_\alpha \frac{\hat{c}_\alpha \hat{b}_\alpha s}{s^2 + 2\zeta_\alpha \omega_\alpha s + \omega_\alpha^2}$$

This will be positive real when $\hat{c}_\alpha \hat{b}_\alpha > 0$, $\alpha = 1, 2, 3, \cdots$. Hence, small errors in collocation of the actuator and sensor can be tolerated without losing the positive real property.

With a view to constructing a state-space model of the system, define the matrices

$$\begin{aligned} &\boldsymbol{\eta} = \mathrm{col}\{\eta_\alpha\}, \quad \boldsymbol{\Omega} = \mathrm{diag}\{\omega_\alpha\}, \\ &\widehat{\mathbf{D}} = \mathrm{diag}\{2\zeta_\alpha \omega_\alpha\}, \quad \widehat{\mathbf{B}} = \mathrm{col}\{\hat{b}_\alpha\} \end{aligned}$$

Then the modal equations in (10) and the output equation in (11) can be represented by the model

$$\dot{\mathbf{x}} = \mathbf{A}\mathbf{x} + \mathbf{B}u + \mathbf{w} \tag{12}$$

$$y = \mathbf{C}\mathbf{x} + v \tag{13}$$

where

$$x = \begin{bmatrix} \dot{\boldsymbol{\eta}} \\ \boldsymbol{\Omega}\boldsymbol{\eta} \end{bmatrix}, \quad A = \begin{bmatrix} -\widehat{\mathbf{D}} & -\boldsymbol{\Omega} \\ \boldsymbol{\Omega} & \mathbf{O} \end{bmatrix}, \quad \mathbf{B} = \mathbf{C}^T = \begin{bmatrix} \widehat{\mathbf{B}} \\ \mathbf{O} \end{bmatrix}$$

Note that we have also introduced a plant disturbance vector $\mathbf{w}$ and sensor noise v. These are largely fictitious and used to support the LQG controller design in the next section.

Our primary motivation in introducing modal coordinates is the ability to systematically reduce the order of the plant model used for controller design. Clearly, a reduced order controller has many advantages from the point of view of real-time implementation. Also, the robust stabilization of a positive real system provided by an SPR controller is independent of the controller order.

CONTROLLER DESIGN

The proposed controller structure consists of a dynamic LQG controller which possesses the SPR property. In the frequency domain,

$$u(s) = -H(s)y(s), \quad H(s) = \mathbf{K}_c(s\mathbf{I} - \mathbf{A}_c)^{-1}\mathbf{K}_e \tag{14}$$

where

$$\mathbf{A}_c = \mathbf{A} - \mathbf{B}\mathbf{K}_c - \mathbf{K}_e\mathbf{C} \tag{15}$$

$$\mathbf{K}_c = \mathbf{R}^{-1}\mathbf{B}^T\mathbf{P}_c \tag{16}$$

$$\mathbf{K}_e = \mathbf{P}_e\mathbf{C}^T\mathbf{R}_v^{-1} \tag{17}$$

and $\mathbf{P}_c$ and $\mathbf{P}_e$ are the solutions of the Riccati equations

$$\mathbf{P}_c\mathbf{A} + \mathbf{A}^T\mathbf{P}_c - \mathbf{P}_c\mathbf{B}\mathbf{R}^{-1}\mathbf{B}^T\mathbf{P}_c + \mathbf{Q} = \mathbf{O} \tag{18}$$

$$\mathbf{P}_e\mathbf{A}^T + \mathbf{A}\mathbf{P}_e - \mathbf{P}_e\mathbf{C}^T\mathbf{R}_v^{-1}\mathbf{C}\mathbf{P}_e + \mathbf{Q}_w = \mathbf{O} \tag{19}$$

Here, $\mathbf{Q} = \mathbf{Q}^T > \mathbf{O}$ and $\mathbf{R} = \mathbf{R}^T > \mathbf{O}$ are the state and control weighting matrices, respectively, which occur in the corresponding LQR problem. $\mathbf{R}_v = \mathbf{R}_v^T > \mathbf{O}$ and $\mathbf{Q}_w = \mathbf{Q}_w^T \geq \mathbf{O}$ are the intensity matrices corresponding to the Gaussian white noises v and $\mathbf{w}$, respectively. It is assumed that $(\mathbf{Q}_w^{1/2}, \mathbf{A})$ is observable.

Since $H(s)$ in Equation (14) is strictly proper, then according to Ioannou and Tao (1987), it is SPR if and only if

(i) $H(s)$ is real for real s and $H(s)$ is analytic for $\mathrm{Re}\{s\} \geq 0$;

(ii) $\mathrm{Re}\{H(j\omega)\} > 0, \quad -\infty < \omega < \infty;$
(iii) $\lim_{\omega\to\infty} \omega^2 \mathrm{Re}\{H(j\omega)\} > 0.$

A time domain characterization of the SPR property uses the triplet $(\mathbf{A}_c, \mathbf{K}_e, \mathbf{K}_c)$ (assumed minimal) and is known as the Kalman-Yakubovich Lemma (Ioannou and Tao, 1987; Wen, 1988): the system $H(s)$ is SPR if and only if there exists positive-definite matrices $\mathbf{P}_0$ and $\mathbf{Q}_0$ such that

$$\mathbf{P}_0\mathbf{A}_c + \mathbf{A}_c^T\mathbf{P}_0 = -\mathbf{Q}_0, \quad \mathbf{P}_0\mathbf{K}_e = \mathbf{K}_c^T$$

Lozano-Leal and Joshi (1988) have shown that if $\mathbf{Q}$, $\mathbf{R}$, $\mathbf{Q}_w$, and $\mathbf{R}_v$ are selected so that

$$\begin{aligned} \mathbf{R}_v &= \mathbf{R} \\ \mathbf{Q} - \mathbf{B}\mathbf{R}^{-1}\mathbf{B}^T &= \mathbf{Q}_b = \mathbf{Q}_b^T > \mathbf{O} \\ \mathbf{Q}_w &= \mathbf{Q}_a + \mathbf{B}\mathbf{R}^{-1}\mathbf{B}^T, \quad \mathbf{Q}_a = -(\mathbf{A} + \mathbf{A}^T) \end{aligned}$$

then the controller $H(s)$ in (14) is SPR. Note that $\mathbf{Q}_b$ and $\mathbf{R}$ are free (positive-definite) design parameters.

SIMULATION RESULTS

For our numerical example, we consider an aluminum box $(E = 70\,\mathrm{GPa}, \quad \rho = 2700\,\mathrm{kg/m^3}, \quad \nu = 0.33)$ with dimensions $a \times b \times c = 1\,\mathrm{m} \times 1.25\,\mathrm{m} \times 1.5\,\mathrm{m}$ and thickness $h = 1\,\mathrm{mm}$. The number of finite elements in the X, Y, and Z directions are 4, 5, and 6, respectively, which leads to square elements of identical size. The finite element mesh and the location of the actuator/sensor combination are illustrated in Figure 2. The first eight vibration mode shapes (neglecting the six rigid body modes) are shown in Figure 3 along with the corresponding vibration frequencies. The properties of the actuator/sensor are given by $e_{31}^0 = 59.1\,\mathrm{N/m/V}$ and $e_{32}^0 = 24.5\,\mathrm{N/m/V}$. The thickness of each layer is $h_a = 28 \times 10^{-6}$ m.

For purposes of the simulation, it will be assumed that the elastic behavior of the system is described by Equations (12) and (13) where the model is constructed using $N = 20$ modes. This is designed to act as a truth model and demonstrate the lack of spillover problems which can occur when higher order modes are destabilized by a lower order controller. The damping ratio for each mode is set at $\zeta = 0.01$. It is assumed that the controller is designed using a reduced number of modes given by $N_c = 5$. Hence the matrices $(\mathbf{A}, \mathbf{B}, \mathbf{C})$ in Equations (15)–(19) are of reduced dimension relative to those in Equations (12) and (13). The SPR controller is designed using the values $R = 5 \times 10^{-5}$ and $\mathbf{Q}_b = \mathbf{I}$. The choice of $\mathbf{Q}_b$ was made so that the corresponding term in the LQR cost function, $(1/2)\mathbf{x}^T\mathbf{Q}_b\mathbf{x}$ is equal to

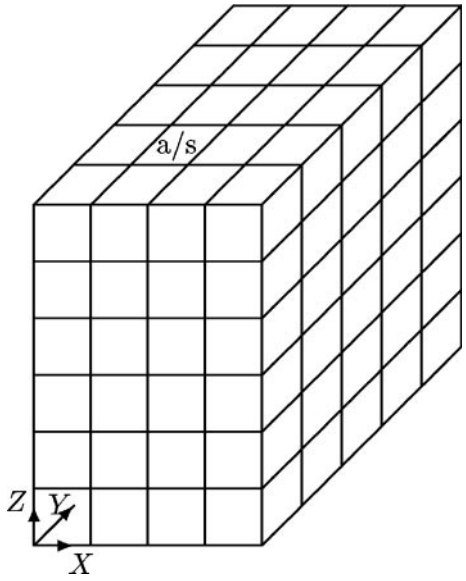

Figure 2. *Finite element mesh with sensor/actuator location.*

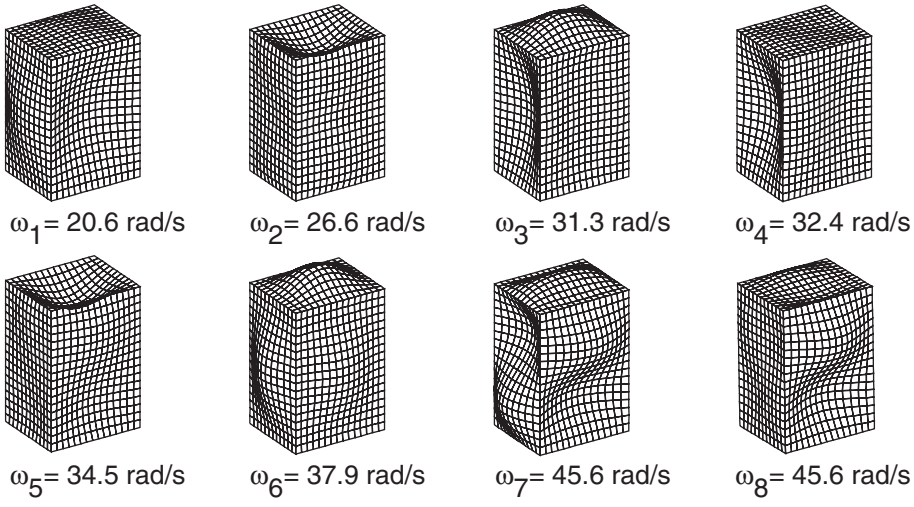

Figure 3. *Box mode shapes.*

the sum of the kinetic and potential (strain) energies in the modeled modes. The scalar R was selected to maximize the damping injected into the first mode and as shown below is close to minimizing the time integral of this energy measure.

Prior to enabling the control system, the box is subject to a disturbance force $d(t)$ acting normal to the box surface at $(X, Y, Z) = (0.5, 0.5, 0)$ m. For this situation, $\mathbf{w}$ in (12) can be written as $\mathbf{w} = \mathbf{B}_d d(t)$ where

$$\mathbf{B}_d = \begin{bmatrix} \widehat{\mathbf{B}}_d \\ \mathbf{0} \end{bmatrix}, \quad \widehat{\mathbf{B}}_d = \text{col}\{\mathbf{q}_\alpha^T \mathbf{b}_d\}$$

where $\mathbf{b}_d$ is a column of zeroes with the exception of a single one located at the degree of freedom where the disturbance is applied. With quiescent initial conditions, the state-space motion equation is integrated for 6 s with

$$d(t) = [1000\sin(1.2t) + 2500\sin t + 1000\sin(0.6t) + 5\sin(0.3t)]N$$

The state vector obtained after 6 s is then used as an appropriate initial condition for the controlled plant. Letting $\mathbf{x}_c$ correspond to the state of the controller in Equation (14), the coupled box and controller equations are given by

$$\begin{bmatrix} \dot{\mathbf{x}} \\ \dot{\mathbf{x}}_c \end{bmatrix} = \begin{bmatrix} \mathbf{A} & -\mathbf{B}\mathbf{K}_c \\ \mathbf{K}_e\mathbf{C} & \mathbf{A}_c \end{bmatrix} \begin{bmatrix} \mathbf{x} \\ \mathbf{x}_c \end{bmatrix} \tag{20}$$

Zero initial conditions are used for the controller states.

The performance of the controller is determined by monitoring the transverse deflection $w(t)$ at three locations corresponding to nodes of the finite element mesh. Hence w can be related to the state vector using

$$w(t) = \mathbf{C}_z\mathbf{x}, \quad \mathbf{C}_w = [\mathbf{0}\ \hat{\mathbf{C}}_w], \quad \hat{\mathbf{C}}_w = \text{row}\{\mathbf{q}_\alpha^T \mathbf{c}_w/\omega_\alpha\} \tag{21}$$

where $\mathbf{c}_w$ is a column of zeroes with the exception of a single one located at the degree of freedom corresponding to where the measurement is made. The three locations are located on orthogonal faces at (0.5, 0, 0.5) m, (1, 0.75, 0.5) m, and (0.5, 0.5, 0) m, the last of which is the location of the disturbance.

The open- and closed-loop responses at the three locations are shown in Figures 4–6. The controller clearly injects damping into the vibration response and there are no signs of spillover instabilities. The control signal, $u(t)$, is depicted in Figure 7. In order to determine

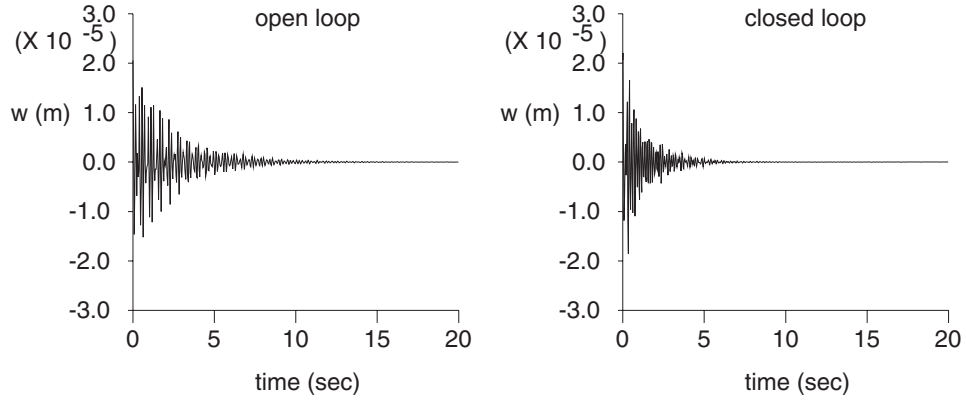

Figure 4. *Response at* $(X, Y, Z) = (0.5, 0, 0.5)\,m$.

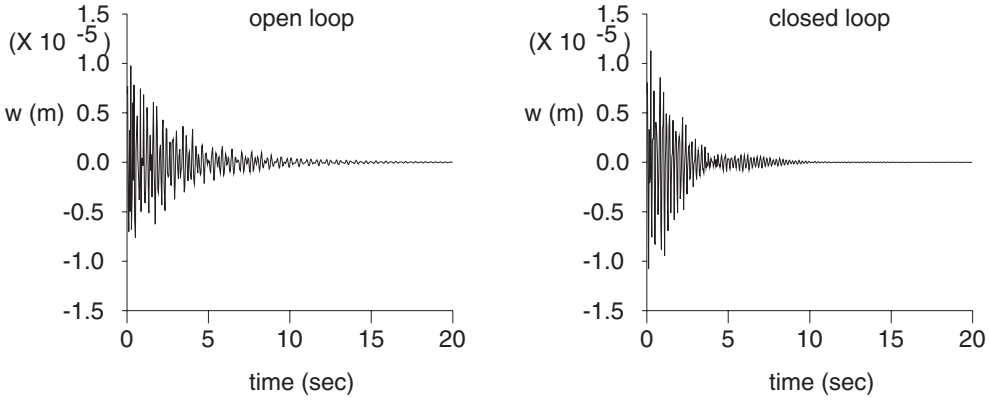

Figure 5. *Response at* $(X, Y, Z) = (1, 0.75, 0.5)\,m$.

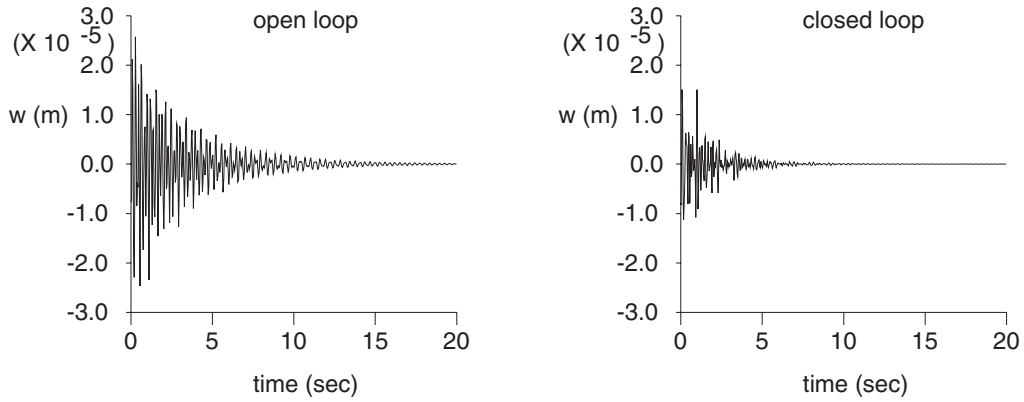

Figure 6. *Response at* $(X, Y, Z) = (0.5, 0.5, 0)\,m$.

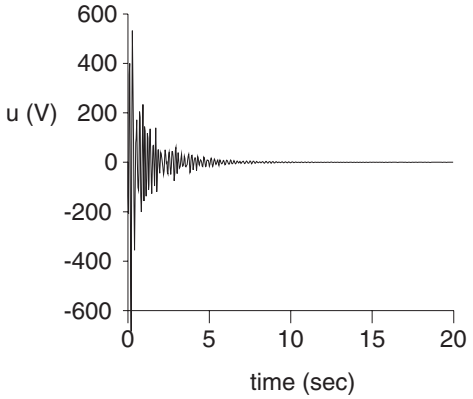

Figure 7. *Control signal u(t).*

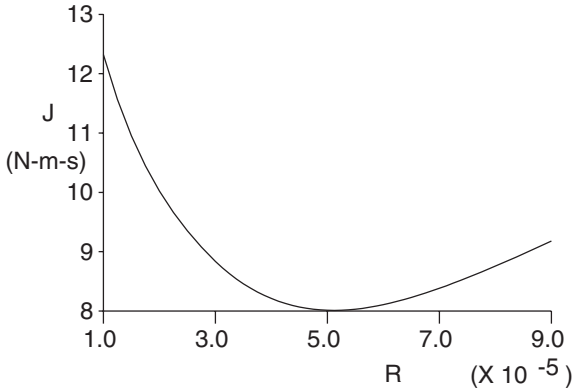

Figure 8. *Energy integral J vs. R.*

the effect of the control weighting R on the controller performance, the integral of energy measure

$$J = \frac{1}{2}\int_0^T \mathbf{x}^T\mathbf{x}\,dt, \quad T = 20\,\text{s}.$$

was calculated for varying R. A plot of J versus R is given in Figure 8 and clearly shows the superiority of our original choice of R.

CONCLUDING REMARKS

We have examined the vibration control of a flexible box structure using a single collocated piezoelectric sensor and actuator pair. Robustness with respect to unmodeled modes was achieved by using an LQG design which also possessed the SPR property. The simulation results showed that it was possible to obtain good damping of the elastic response to a disturbance.

REFERENCES

Bailey, T. and Hubbard Jr., J.E. 1985. "Distributed Piezoelectric-Polymer Active Vibration Control of a Cantilever Beam," *Journal of Guidance, Dynamics, and Control*, 8(5):605–611.

Baz, A. and Ro, J. 1996. "Vibration Control of Plates with Active Constrained Layer Damping," *Smart Mater. Struct.*, 5:372–280.

Benhabib, R.J., Iwens, R.P. and Jackson, R.L. 1981. "Stability of Large Space Structure Control Systems Using Positivity Concepts," *AIAA J. Guidance and Control*, 4(5):487–494.

Crawley, E.F. and de Luis, J. 1987. "Use of Piezoelectric Actuators as Elements of Intelligent Structures," *AIAA J.*, 25(10):1373–1385.

Desoer, C.A. and Vidyasagar, M. 1975. *Feedback Systems: Input-Output Properties*, Academic Press, New York.

Halim, D. and Moheimani, S.O.R. 2002. "Experimental Implementation of Spatial H-infinity Control on a Piezoelectric-Laminate Beam," *IEEE-ASME Trans. Mechatronics*, 7:346–356.

Ioannou, P. and Tao, G. 1987. "Frequency Domain Conditions for Strictly Positive Real Functions," *IEEE Trans. Automat. Control*, 32:53–54.

Lee, C.K. 1990. "Theory of Laminated Piezoelectric Plates for the Design of Distributed Sensors/actuators. Part I: Governing Equations and Reciprocal Relationships," *J. Acoust. Soc. Am.*, 87(3):1144–1158.

Lozano-Leal, R. and Joshi, S.M. 1988. "On the Design of Dissipative LQG-Type Controllers," *Proc. 27th IEEE Decision and Control Conference*, 2:1645–1646.

Sun, D.C., Tong, L.Y., and Wang, D.J. 2001. "Vibration Control of Plates Using Discretely Distributed Piezoelectric Quasi-modal Actuators/sensors," *AIAA J.*, 39:1766–1772.

Wang, S.Y., Quek, S.T., and Ang, K.K. 2001. "Vibration Control of Smart Piezoelectric Composite Plates," *Smart Mater. Struct.*, 10:637–644.

Wen, J.T. 1988. "Time Domain and Frequency Domain Conditions for Strict Positive Realness," *IEEE Trans. Automatic Control*, 33(10):988–992.